Nuclear Engineering and Technology 54 (2022) 2359–2366

Contents lists available at ScienceDirect

Nuclear Engineering and Technology

journal homepage: www.elsevier.com/locate/net

Original Article

Comparison of the effects of irradiation on iso-molded, fine grain nuclear graphites: ETU-10, IG-110 and NBG-25

Se-Hwan Chi

Global Institute for Nuclear Initiative Strategy (GINIS), 302 Nutopia Bd., Yuseong-gu, Daejeon, 34166, South Korea

ARTICLE INFO

Article history:
Received 3 September 2021
Received in revised form
12 December 2021
Accepted 3 January 2022
Available online 5 January 2022

Keywords:
Fine grain iso-molding
Nuclear graphite
Radiation effects
Volume change (VC)
Thermal conductivity (TC)
Dynamic Young's modulus (DYM)
Co-efficient of thermal expansion (CTE)

ABSTRACT

Selecting graphite grades with superior irradiation characteristics is important task for designers of graphite moderation reactors. To provide reference information and data for graphite selection, the effects of irradiation on three fine-grained, iso-molded nuclear grade graphites, ETU-10, IG-110, and NBG-25, were compared based on irradiation-induced changes in volume, thermal conductivity, dynamic Young's modulus, and coefficient of thermal expansion. Data employed in this study were obtained from reported irradiation test results in the high flux isotope reactor (HFIR)(ORNL) (ETU-10, IG-110) and high flux reactor (HFR)(NRL) (IG-110, NBG-25). Comparisons were made based on the irradiation dose and irradiation temperature. Overall, the three grades showed similar irradiation-induced property change behaviors, which followed the historic data. More or less grade-sensitive behaviors were observed for the changes in volume and thermal conductivity, and, in contrast, grade-insensitive behaviors were observed for dynamic Young's modulus and coefficient of thermal expansion changes. The ETU-10 of the smallest grain size appeared to show a relatively smaller VC to IG-110 and NBG-25. Drastic decrease in the difference in thermal conductivity was observed for ETU-10 and IG-110 after irradiation. The similar irradiation-induced properties changing behaviors observed in this study especially in the DYM and CTE may be attributed to the assumed similar microstructures that evolved from the similar size coke particles and the same forming method.

1. Introduction

Currently there are more than 70 small modular reactor (SMR) designs under development for different applications in all principal reactor lines: water cooled reactors, high temperature gas cooled reactors, liquid-metal, sodium and gas cooled reactors with fast neutron spectrum, and molten salt reactors. The key driving forces of these SMR developments are being discussed based on their flexible power generation and wide application, offering better economic affordability [1,2].

It is worth noting that, of these SMRs under development, at least 16 designs are high temperature gas-cooled reactor (HTGR) and 10 reactors are molten salt reactors (MSR) with potential graphite moderation. In these SMRs, graphite will be used for the construction of major core components including the fuel block and reflector. These graphite core components will be subjected to neutron irradiation under high temperature helium (He) gas coolant or molten salt environments, resulting in changes to the graphite microstructure, dimensions, and physical constants, including Young's modulus, thermal conductivity, coefficient of thermal expansion, etc. It is well known that these changes in the physical and thermal properties of graphite core components degrade the integrity of the components, endangering the safety of the reactor [3]. Thus, for designers of graphite moderation reactors, selecting graphite grades with superior irradiation characteristics is important. For this, they need various data, including irradiation test data, to select among the candidates by comparison. However, irradiation data for comparison, especially for fine-grained, isotropic or near-isotropic grades, are limited.

In this study, to provide reference information and data necessary in graphite selection for graphite core components designers, the effects of irradiation on three fine-grained, iso-molded nuclear graphite grades, ETU-10, IG-110, and NBG-25, were compared based on the irradiation-induced changes in their volume (VC), thermal conductivity (TC), dynamic Young's modulus (DYM), and coefficient of thermal expansion (CTE). The data compared in this study were obtained from the reported high flux isotope reactor

E-mail address: shchi5301@gmail.com.

https://doi.org/10.1016/j.net.2022.01.008

(HFIR) irradiation test results (ORNL) (ETU-10, IG-110) [4–9] and high flux reactor (HFR) (NRL, Petten) irradiation test results (IG-110, NBG-25) [10]. Comparisons were made based on the irradiation dose (dpa) and irradiation temperature.

2. Materials and irradiation conditions

Table 1 compares the major characteristics and properties of ETU-10, IG-110, and NBG-25 nuclear grade graphite with those of the ASTM D 7219-08 Standard Specification for Isotropic and Near-isotropic Nuclear Graphite [11]. Table 1 shows that all three grades, which were produced by the same iso-molding forming method using fine size coke particles, satisfied the ASTM D 7219-08 requirements and showed little difference in their physical properties, except grain size and thermal conductivity. While all three grades met the ASTM D 7219-08 specification requirement for a TC of 90 W/m°K, the ETU-10 with the smallest grain size appeared to have the smallest TC among the grades. Relatively smaller differences in the DYM and CTE were observed among the grades.

Table 2 compares the four reactor irradiation test conditions, dose (dpa) and irradiation temperature (°C), from which all the data compared in this study were obtained. Table 2 shows that all the data compared in this study were produced from two reactors: the high flux isotope reactor (HFIR) in Oak Ridge National Laboratory (ORNL), USA, and the high flux reactor (HFR) in the nuclear research laboratory (NRL), Petten, Netherland. It is seen in Table 2 that HFIR produced the irradiation data for ETU-10, hereafter designated HFIR (ETU-10), and two irradiation data for the IG-110 in 1996, hereafter HFIR (IG-110) 1996, and in 2017, hereafter HFIR (IG-110) 2017. HFR produced the irradiation data for 8 different grades including IG-110 and NBG-25 during the INNOGRAPH project, from which the irradiation data of the IG-110, hereafter HFR (IG-110), and of the NBG-25, hereafter HFR (NBG-25) were compared with those of the HFIR (ETU-10), the HFIR (IG-110, 1996), and the HFIR (IG-110, 2017).

It is worth noting in Table 2 that the irradiation temperatures and doses of the four irradiation tests are not the same. For HFIR (IG-110, 2017), while all of the specimens were irradiated at the 600 °C target temperature, the actual irradiation temperatures estimated for each specimen were different than the target temperature. The estimated individual temperature for each specimen was reported [7] and is used in this study for comparison instead of the target temperature, as necessary.

It is worth noting that the irradiation conditions in dpa between the HFIR (ETU-10) and HFIR (IG-110, 2017) were nearly the same. Thus, the difference in dpa between the two reactor irradiations was 0.4 dpa at $40x10^{25}$ nm^{-2} (E > 0.5 MeV). However, the differences in the irradiation temperature and fluence (dpa) in the reactor irradiation tests in Table 2 imply that the present comparison study is of “qualitative” rather than “quantitative” nature.

Table 3 compares the four irradiation tests based on the data produced. Based on this Table 3, the changes in volume (VC), thermal conductivity (TC), dynamic Young's modulus (DYM), and coefficient of thermal expansion (CTE) data were selected for the comparison of irradiation effects on ETU-10, IG-110, and NBG-25 in this study.

3. Comparison of the irradiation effects on ETU-10, IG-110 and NBG-25

3.1. Volume Change (VC)

Fig. 1 compares the irradiation-induced volume change behaviors, i.e., ($\triangle V/V_o$, %)-dpa between the HFIR (ETU-10), the HFIR (IG-110, 1996) and the HFIR (IG-110, 2017). Fig. 2 compares the volume change behaviors with irradiation of the HFIR (ETU-10), the HFR (IG-110) and the HFR (NBG-25). Here, HFR (IG-110) and HFR (NBG-25) refer to the volume change curves of the IG-110 and NBG-25 in the HFR irradiated 8 grades in the EU INNOGRAPH project, respectively [10]. In Fig. 1, it is worth noting that each HFIR (IG-110, 2017) data point represents an average of two or three VC data at the estimated individual irradiation temperature, as detailed in Table 4. Fig. 1 shows that the turn-around and cross-over behaviors between the HFIR (ETU-10) and the HFIR (IG-110, 2017) are similar, while some differences can be observed between these two and the HFIR (IG-110, 1996). Table 5 summarizes the predicted turn-around dimensional change (contraction %) and cross-over dose (dpa) from Fig. 1, where the maximum dimensional change (contraction) of HFIR (ETU-10), −4%, appears to be smaller than those of the HFIR (IG-110, 2017), −6.3%, and the HFIR (IG-110, 1996), −7%.

Here, it is worth noting in Table 4 that the two estimated individual irradiation temperatures, i.e., 667 °C at 10.8 dpa and 667 °C at 20.5 dpa in HFIR (IG-110, 2017) are higher than the 600 °C target temperature of the HFIR (IG-110, 2017), respectively. From this temperature distribution in the HFIR (IG-110, 2017), it is predicted that the irradiation temperature of the HFIR (IG-110, 2017) VC specimens will be higher than HFIR (ETU-10), 598 °C. This prediction implies that there will be a further decrease in the volume contraction in the ETU-10 if the ETU-10 is irradiated together with the IG-110 and the NBG-25 in the HFIR (IG-10, 2017) of 639 ± 36 °C [7].

Fig. 2 shows that, while the cross-over dpa of the HFIR (ETU-10) is predicted to be somewhat larger than those of the HFR (IG-110) and HFR (NBG-25), overall, the turn-around behaviors of the HFIR (ETU-10), the HFR (IG-110), and the HFR (NBG-25) appear similar each other at around 11–12 dpa and − 5% contraction. However, if the difference in the irradiation temperature between them is considered, i.e., 598 °C for the HFIR (ETU-10) and 750 °C for the HFR (IG-110) and the HFR (NBG-25), it is predicted that, if the ETU-10 was included in the HFR (INNOGRAPH project) at 750 °C

Table 1
Comparison of the major characteristics and properties of ETU-10, IG-110, and NBG-25 nuclear graphite grades with those of ASTM D 7219-08 Standard Specification for Isotropic and Near-isotropic Nuclear Graphite. All property data for the ETU-10, IG-110, and NBG-25 were obtained from manufacturer's data sheet, except for the grain size of IG-110.

	ASTM D-7219-08 [11]	ETU-10	IG-110	NBG-25
Manufacturer	N/A	Ibiden	Toyo Tanso	SGL
Cokes Type	N/A	Pitch	Petro	Petro
Forming method		Iso-molding	Iso-molding	Iso-molding
CTE Isotropy Ratio (αAG/αWG)	1.0–1.1	1.08	1.09	1.10
Bulk Density (g/cm^3) (min)	1.70	1.75	1.77	1.82
Grain size (μm)	Generally<100 μm	15	20-40 [10]	Max. 60
Thermal Conductivity at 25 °C, AG, Wm^{-1} °K^{-1} (min)	90	104	130	140
Dynamic Young's Modulus, WG, GPa	8-15	10.8	9.7	11.0
Coefficient of Thermal Expansion (25–500 °C), WG, X 10^{-6} °C^{-1}	3.5–5.5	3.8 (50–400 °C)	4.5	3.9 (20–200 °C)

Table 2
The four nuclear graphite irradiation tests compared in this study.

Reactor	High Flux Isotope Reactor (HFIR)*			High Flux Reactor (HFR)**
Irradiation Grade	ETU-10	IG-110 (1996)	IG-110 (2017)	IG-110, NBG-25, and other 6 grades
Irradiation Temp.	342–667 °C	600 °C	639 ± 36 °C	750 °C, 950 °C
dpa	3–30	~25	5–30	4.1–25 (750 °C) 15 (950 °C)
Remark-1	598 °C and 667 °C irradiation data were used for comparison with HFIR (IG-110) and HFR (IG-110, NBG-25), respectively.		Data from 600 °C tar-get temperature were used for comparison with IG-110 (1997) and ETU-10.	IG-110, NBG-10, -17, −18, −25, PCEA, PCIB, PPEA were irradiated together in the INNOGRAPH project. Data from 750 °C irradiation were used in this study.
Remark-2	HFIR (ETU-10)	HFIR (IG-110, 1996)	HFIR (IG-110, 2017)	HFR (IG-110), HFR (NBG-25)
Reference	[8]	[4]	[5–7]	[10]

*HFIR: High Flux Isotope Reactor (Oak Ridge National Lab., Oak Ridge, USA).
**HFR: High Flux Reactor (Nuclear Research Laboratory, Petten, The Netherland).

Table 3
Comparison of reported data produced from the reactor irradiation tests. Based on this comparison, the dimensional change (DC), thermal conductivity (TC), elastic modulus (dynamic young's modulus) (DYM), and coefficient of thermal expansion (CTE) data were selected to compare the irradiation effects on ETU-10, IG-110, and NBG-25 in this study.

	HFIR (ETU-10)	HFIR (IG-110, 1996)	HFIR (IG-110, 2017)	HFR (IG-110, NBG-25)
Dimensional change	○	○	○	○
Thermal conductivity	○	○	○	○
Elastic modulus	○	○	○	○
Coefficient of thermal expansion	○	X	○	○
Electrical resistivity	X	○	X	X
Fracture strength	X	○	X	X
Four-point flexure strength	X	X	○	X
Tensile strength	X	X	X	○
Creep	X	X	○	X
Reference	[8]	[4]	[5–7]	[10]

irradiation temperature, the dimensional change and the cross over dpa of the HFR (ETU-10) could be smaller than the HFIR (ETU-10), the HFR (IG-110) and the HFR (NBG-25) owing to the irradiation temperature effects on dimensional change.

3.2. Thermal Conductivity (TC)

Table 6 compares the un-irradiated and irradiated TCs, together with the decrease in TC (%) from the un-irradiated TC in parenthesis produced by irradiation, for the HFIR (ETU-10), the HFIR (IG-110, 1996), and the HFIR (IG-110, 2017). Large differences can be observed in the un-irradiated TC of the HFIR (ETU-10), the HFIR (IG-110, 1996) and the HFIR (IG-110, 2017). After irradiation, however, a drastic decrease in the differences in TC between the grades was observed: Thus, from 56 W/m°K to 6.5 W/m°K in the un-irradiated condition and in the irradiation condition (24.8 dpa) between the HFIR (ETU-10) and HFIR (IG-110, 1996), respectively.

Further, it is worth noting the similar rate of decrease in TCs after irradiation of the HFIR (ETU-10) and HFIR (IG-110, 1996) up to ~ 25 dpa. A related analysis showed that the TC of HFIR (ETU-10) was 16–25 W/mK at 12–20 dpa, and stayed at 16 W/mK for 20–25 dpa.

Fig. 3 compares the irradiation induced changes in the thermal conductivity (TC) of the HFIR (ETU-10) [8,9], the HFR (IG-110) and the HFR (NBG-25) [10]. It is observed that all three curves tend to show similar historic irradiation-induced TC changing behaviors, i.e., a fast decrease in TC with irradiation below 1 dpa, and, of the three grades, the lower TC-dpa behavior in HFIR (ETU-10) is noted for 5–10 dpa with a similar trend to the HFR (NBG-25) at around 15 dpa.

3.3. Dynamic Young's Modulus (DYM)

The DYM-dpa relationship of the HFIR (ETU-10) [8], the HFIR (IG-110, 2017) [5,7] and the HFIR (IG-110, 1996) [4] is compared in Fig. 4 and of the HFIR (ETU-10) [8,9], the HFR (IG-110) and the HFR (NBG-25) [10] is compared in Fig. 5, respectively. Fig. 4 shows that the irradiation-induced DYM behaviors, i.e., E/Eo – dpa, of the HFIR (ETU-10) and HFIR (IG-110, 1996) are similar to each other, showing a higher value than the HFIR (IG-110, 2017) of about 10%–65% at 3–20 dpa. These irradiation-induced DYM changing behaviors are typical in that they show an increase in DYM with irradiation (dpa) up to the peak value (E/Eo ~ 2.5) [14,15]. Though limited data are available for the HFIR (IG-110, 2017), the large difference in the E/Eo – dpa behavior of the HFIR (IG-110, 1996) and the HFIR (IG-110, 2017) of the same grade and same reactor irradiation is noted. It is seen that all three grades show a large increase in E/Eo at around their turn-around doses, 9–15 dpa (Table 5).

In Fig. 5, after an initial fast rise with irradiation below 3 dpa, both the HFIR (ETU-10) and HFR (IG-110) tend to show similar DYM-dpa behavior up to about 13 dpa, nearing both grades' turn-around, Table 5, forming a lower boundary in the HFR (INNOGRAPH project) DYM-dpa data. For 13 - 25 dpa, similar DYM-dpa behaviors are noted for the HFIR (ETU-10) and the HFR (NBG-25). Regarding the relationship between the DYM-dpa behavior and the turn-around dose, even though the HFIR (ETU-10), the HFR (IG-110) and the HFR (NBG-25) show similar DYM-dpa behaviors, the higher DYM-dpa behaviors of the HFIR (ETU-10) and the HFR (NBG-25) over the HFR (IG-110) is noted after the turn-around dose of the HFIR (IG-110), 9–15 dpa.

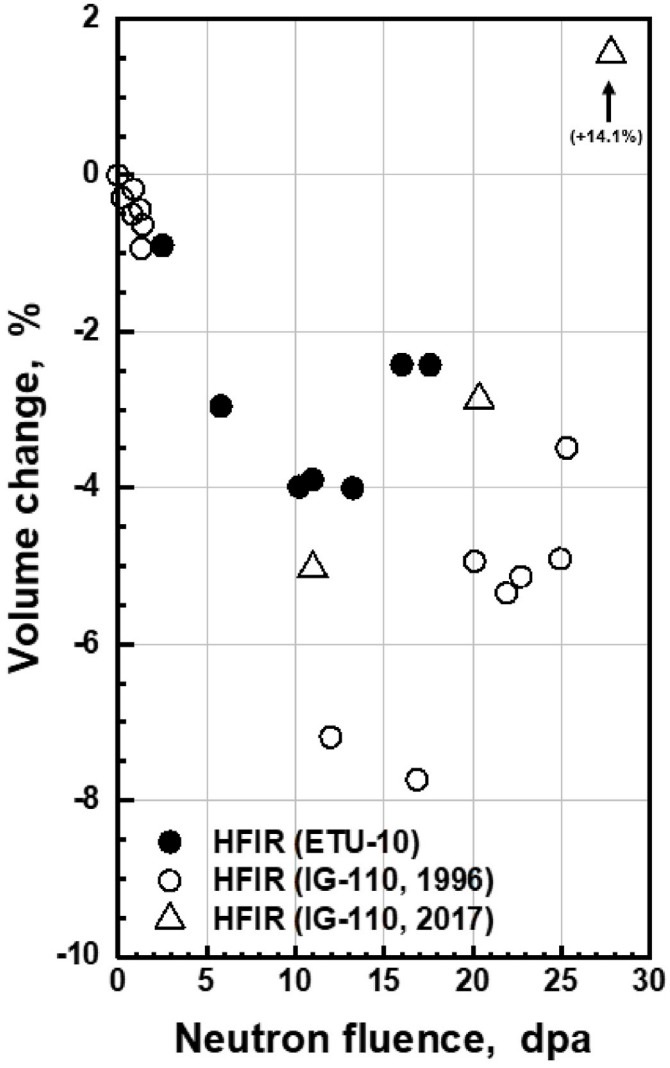

Fig. 1. Comparison of the volume change behaviors with neutron dose of the HFIR (ETU-10) [8], the HFIR (IG-110, 2017) [5–7] and the HFIR (IG-110, 1996) [4]. Irr. Temp.: HFIR (ETU-10) (598°C), HFIR (IG-110, 1996) (600°C), HFIR (IG-110, 2017) (639±36°C).

3.4. Coefficient of Thermal Expansion (CTE)

The irradiation-induced CTE behaviors of the HFIR (ETU-10) (598 ± 51 °C, TR) and the HFIR (IG-110, 2017) (design temperature: 600 °C, measured temperature: 588 °C, 662 °C, 667 °C,TR) are compared in Fig. 6. No CTE-dpa data are available from the HFIR (IG-110, 1996), Table 3. Here, detailed information about the three HFIR (IG-110, 2017) data is shown in Table 7, which shows that the measured actual temperatures, 588 °C, 662 °C, and 667 °C, differ from the target irradiation temperature (design temperature), 600 °C, in HFIR (IG-110, 2017) [5,6]. Fig. 6 shows the surprisingly similar CTE-dpa behaviors of the HFIR (ETU-10) (598 °C ± 51 °C, TR) and the HFIR (IG-II0, 2017) (588 °C, 662 °C, 667 °C, TR) showing a historic CTE-dpa trend where, at around 600 °C irradiation temperature, the CTE increases with irradiation showing a peak at around 5 dpa followed by a decrease with irradiation to around 60% of the un-irradiated CTE value at around 25 dpa [16].

Fig. 7 shows a comparison of the CTE-dpa of the HFIR (ETU-10) (irr. temp: 598 °C) [8,9] and the HFR (IG-110), the HFR (NBG-25) in HFR (INNOGRAPH project) (irr. temp: 750 °C) [10].

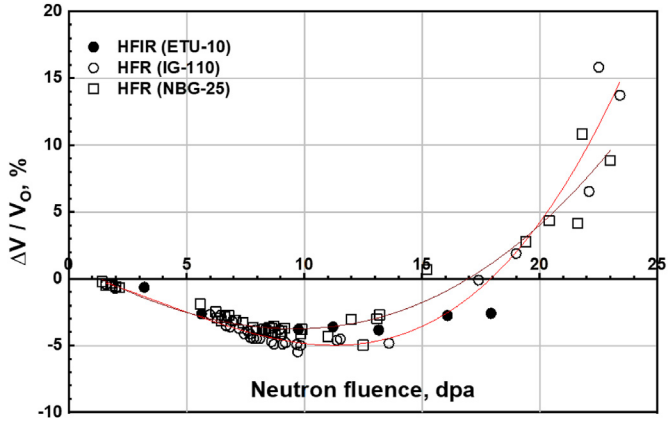

Fig. 2. Comparison of the volume change behaviors with doses of the HFIR (ETU-10) [8] and the HFR (IG-110) and the HFR (NBG-25) [10]. Irr. Temp.: HFIR (ETU-10) (598°C), HFR (IG-110, NBG-25) (750°C).

In Fig. 7, the changes in CTE behaviors with irradiation in the HFR (IG-110), the HFR (NBG-25) and the HFIR (ETU-10) are typical of many fine-textured graphites [16], which undergo an initial increase in the CTE to the peak, 4.5–5.5x10^{-6} K^{-1}, followed by a steady reduction to a value about 60% of the un-irradiated CTE value, 3.0–4.0x10^{-6} K^{-1}. In spite of the difference in the irradiation temperature of the HFIR (ETU-10) of 598 °C, and the HFR (INNOGRAPH project) of 750 °C, it is observed that the HFIR (ETU-10) tends to show CTE-dpa behavior similar to the HFR (IG-110) for <5 dpa and to the HFR (IG-110) and the HFR (NBG-25) for 5–15 dpa.

4. Discussion

The overall similarities in the irradiation-induced volume and properties changes observed in this study for the ETU-10, the IG-110, and the NBG-25 may be because they each had the same forming method, and the same fine size coke particles were employed to produce the three grades. It is well known that several of the physical, thermal, and mechanical properties of graphite are determined largely by the coke particle size and forming method [3,17–19].

Among the properties compared in this study, the irradiation-induced changes in volume (VC) and thermal conductivity (TC) appeared to be more or less grade-sensitive as seen in Fig. 1 and Table 6, and the dynamic young's modulus (DYM) and the coefficient of thermal expansion (CTE) appeared to be more or less grade-insensitive as seen in Figs. 4 and 6. These observations may be compared to the observation made by M.C.R. Heijna et al. during their INNOGRAPH irradiation studies [10,19]. They compared the irradiation behaviors of eight HTR graphite grades manufactured from various grain sizes and forming methods, and found that, among the five properties compared, the CTE and DYM were “similar” across the eight grades compared.

Here, regarding the differences in the irradiation temperature in the reactor irradiation studies compared in this study, i.e., Tables 2 and 5, the effects of irradiation temperature on the irradiation-induced properties changes need to be considered. It has been observed that the irradiation-induced properties changes happen more rapidly at higher irradiation temperature but the severity of the changes are reduced [7]. These observed irradiation temperature effects on properties changes may need to be applied to the present comparison of irradiation-induced properties changes that evolved from the four nuclear graphite irradiation tests of different irradiation temperatures, Table 2.

Table 4
Detailed information of the three HFIR (IG-110, 2017) data points in Fig. 1 [7].

Volume change (%)	X 10^{25} n/m^2 (E > 0.1 MeV)	dpa (Irradiation temperature)
−4.7	14.3 (TR 3 points)	10.8 (667 °C)
−5.1		
−5.0		
TR average: −4.9		
−2.8	27.0 (TR 3 points)	20.5 (667 °C)
−2.9		
−2.4		
TR average: −2.7		
+16.4	37.4 (TR 2 points)	28.3 (588 °C)
+11.8		
TR average: +14.1		

TR: Transverse (to the loading direction during iso-molding process in specimen orientation).

Table 5
Prediction of the turn-around contraction (%) and cross-over dose (dpa) from Fig. 1.

	Turn-around volume contraction (%) and dose (dpa)	Cross-over (dpa)	Irradiation temperature
HFIR (IG-110, 1996)	−7.0 %, 15.0 dpa	30 dpa	600 °C
HFIR (IG-110, 2017)	−6.3 %, 9.2 dpa	20-25 dpa	639 ± 36 °C.
HFIR (ETU-10)	−4.0 %, 10.0 dpa	20-25 dpa	598 °C

Table 6
Comparison of the irradiation-induced thermal conductivity changes of the HFIR (ETU-10), the HFIR (IG-110, 1996) and the HFIR (IG-110, 2017). Unit: W/m°K.

Dose (dpa)	HFIR (ETU-10)	HFIR (IG-110, 1996)	HFIR (IG-110, 2017)
Un-irr	104	160	130
11.9	25.0 (−76.0%)	35.0 (−78.1%)	42.3
21.8	16.0 (−84.6%)	27.5 (−82.8%)	*
24.8	16.0 (−84.6%)	22.5 (−85.9%)	*

* No measurement data available.

For VC, even limited data are available, if the observed irradiation temperature effects are considered, both Figs. 1 and 2 will show a further smaller VC for HFIR (ETU-10) to HFIR (IG-110, 2017) and HFIR (IG-110, 1997) in Fig. 1 and to HFR (IG-110) and HFR (NBG-25) in Fig. 2 at a similar turn-around dpa. It is known that at higher irradiation temperatures, the volume changes happen more rapidly with reduced dimensional changes, especially for molded graphites [7,18].

For TC, Table 6 and Fig. 3 show that all the changes in the irradiation-induced thermal conductivity behaviors are similar to the historical data trend, where fast and large decreases in TC occur as soon as irradiation begins (<1 dpa) regardless of the un-irradiated TC [13,15]. Table 6 also shows that the large difference in the un-irradiated TC of the HFIR (ETU-10) and HFIR (IG-110, 1996) decreases fast with irradiation, i.e., from 56 W/m°K in un-irradiated condition to 11.5 W/m°K (−80.0% decrease) at 21.8 dpa and to 6.5 W//m°K (−88.4% decrease) at 24.8 dpa, respectively. In Table 6, even the irradiation temperature effects on TC are considered, negligible changes are expected owing to the similar irradiation

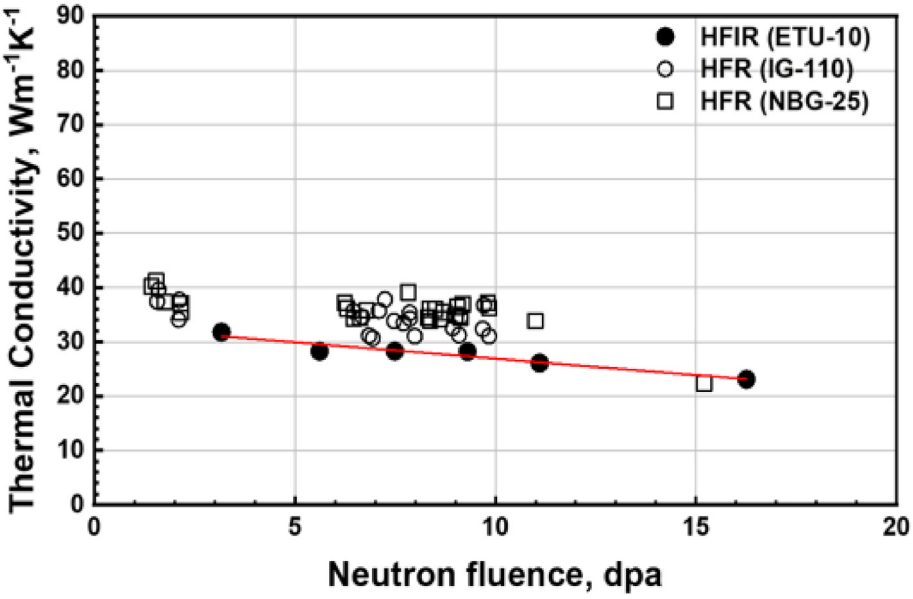

Fig. 3. Comparison of the irradiation-induced changes in TC of the HFIR (ETU-10) [8], the HFR (IG-110) and the HFR (NBG-25) [10]. Irr. Temp.: HFIR (ETU-10) (598°C). HFR (IG-110, NBG-25) (750°C). Un-irradiated TC (W/m°K): ETU-10: 104, IG-110: 130, NBG-25: 140.

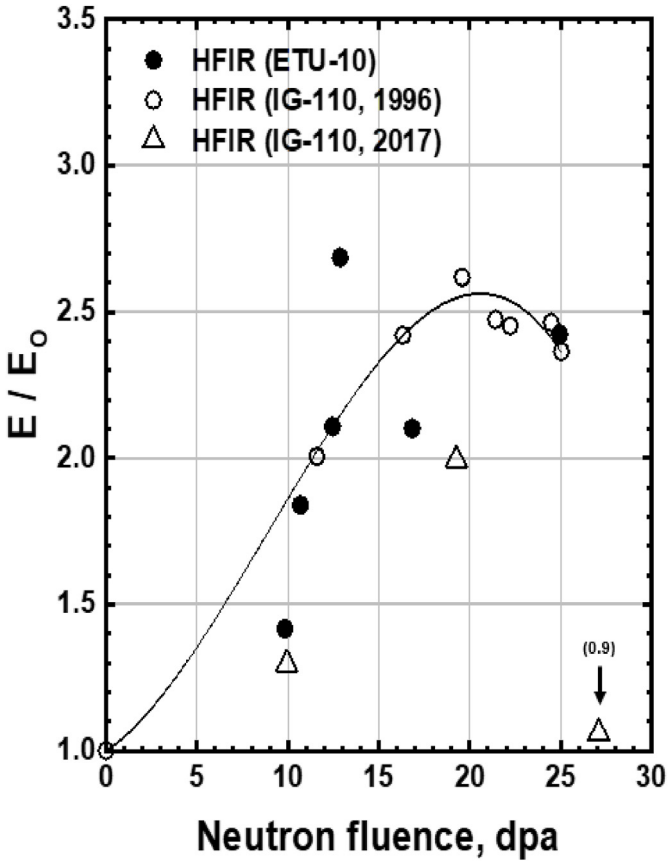

Fig. 4. Comparison of the irradiation-induced changes in the DYM of the HFIR (ETU-10) [8], the HFIR (IG-110, 2017) [5,6], and the HFIR (IG-110, 1996) [4]. Un-irradiated DYM: ETU-10: 9.7–9.8 GPa, IG-110: 9.1–10.2 GPa. Irr. Temp.: HFIR (ETU-10) (598°), HFIR (IG-110, 2017) (639°C±36°C), HFIR (IG-110, 1996) (600°C).

temperature for the HFIR (ETU-10), the HFIR (IG-110, 1996), and the HFIR (IG-110, 2017). However, for HFIR (ETU-10) (Irr. temp: 598 °C) and HFR (INNOGRAPH project) (Irr. temp: 750 °C) in Fig. 3, the irradiation temperature effects on TC may need to be considered during evaluation of Fig. 3. Thus, if the HFIR(ETU-10) (Irr. temp: 598 °C) was irradiated at 750 °C of HFR (INNOGRAPH project)

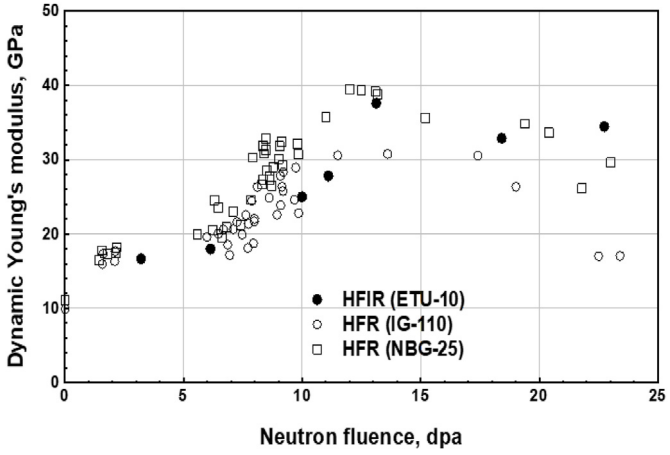

Fig. 5. Comparison of DYM-dpa relationship for the HFIR (ETU-10) [8], the HFR (IG-110) and the HFR (NBG-25) [10]. Irr. Temp.: HFIR (ETU-10) (598°C), HFR (INNOGRAPH project) (750°C).

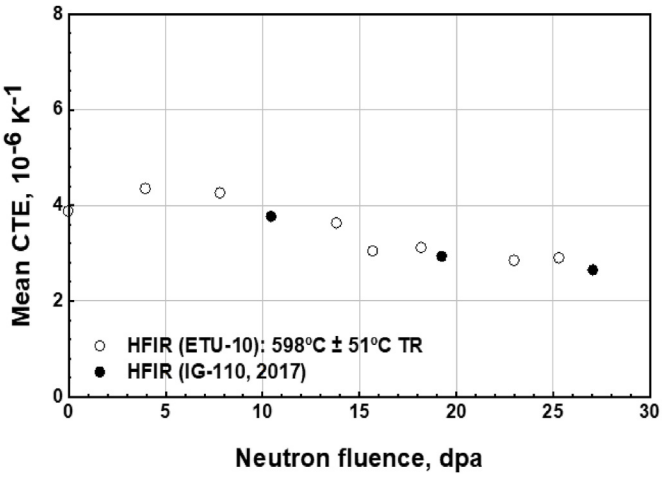

Fig. 6. Comparison of the CTE-dpa behavior of the HFIR (ETU-10) (Irr. Temp.:598°±51°, TR) [8] and the HFIR (IG-110, 2017) (design temperature: 600°C, measured temperature: 588°C, 662°C, 667°C, TR) [5–7]. Un-irradiated CTE (TR): IG-110: 4.5X10^{-6}°K^{-1},ETU-10: 3.8X10^{-6}°K^{-1}.

irradiation temperature, or if the ETU-10 was irradiated together with the IG-110 and the NBG-25 at 750 °C in HFR (INNOGRAPH project), the TC of HFR (ETU-10) (Irr. temp: 750 °C) will show a slightly larger TC than the present TC showing a further similar irradiation-induced TC changing behavior to HFR (IG-110) and HFR (NBG-25) [13]. In Table 1, it was observed that the ETU-10 of the smallest grain size exhibited the smallest TC among the three grades. The relationship between grain size and TC is well established, based on the increased phonon scattering at grain boundaries [20]. Table 6 shows that this relationship between the TC and grain size is maintained even after irradiation, up to about 25 dpa.

In Table 6, the observed similar irradiation-induced TC decreasing behavior between the HFIR (ETU-10) and HFIR (IG-110, 1996) at 11.9–24.8 dpa suggests a similar irradiation-induced lattice defect (a barrier to phonon transport) evolution behavior between the HFIR (ETU-10) and HFIR (IG-110, 1996) [20].

The observed over all similar irradiation-induced DYM (E/Eo) changing behavior between the HFIR (ETU-10) and HFIR (IG-110, 1996) in Fig. 4 and between the HFIR (ETU-10), HFR (IG-110) and HFR (NBG-25) in Fig. 5 may be understood based on the suggested similarity in microstructure and irradiation-induced lattice defect evolution behavior between the grades. The increase in DYM (E/Eo) due to irradiation has been discussed based on the dislocation-pinning by radiation-induced lattice defects in the early stage of irradiation, followed by changes in pore structure (densification) [21]. Fig. 5 also shows that the DYM and differences in DYM among the grades increase with irradiation. The increase in the difference in DYM between the grades may be attributed to the difference in the volume changing behavior after turn-around among the grades. As seen in Table 5 (turn-around dose), Fig. 5 shows that the DYM of each grade peaks at around their turn-around dose and the difference in DYM increases after their turn-around doses, 9–15 dpa, suggesting a difference in the microstructural volume changing behavior such as generation of cracks and pores between the grades after turn-around and across the cross-over [3]. Here, in Fig. 5, if the differences in the irradiation temperature between the HFIR (ETU-10) (Irr. temp: 598 °C), the HFR (IG-110) (Irr. temp: 750 °C) and the HFR (NBG-25) (Irr. temp: 750 °C) are considered, the ETU-10 irradiated together with the IG-110 and NBG-25, i.e., HFR (ETU-10), is predicted to show DYM-dpa behavior that is closer to the HFR (IG-110) and the HFR (NBG-25) since some increase in DYM is excepted if the irradiation temperature increases from 598 °C to 750 °C [14,15].

Table 7
The overlapped three HFIR (IG-110, 2017) CTE data (TR) in Fig. 6 [7].

Design Temperature	Measurement temperature	Fluence ($X10^{25}$ nm^{-2}) (dpa)	Average CTE change for three measured CTE	CTE after irradiation ($X10^{-6}$ K^{-1})
600 °C	667 °C	14.3 (10)	−8.5%	3.84
	662 °C	27.0 (19)	−30.3%	2.93
	588 °C	37.4 (27)	−36.8%	2.65

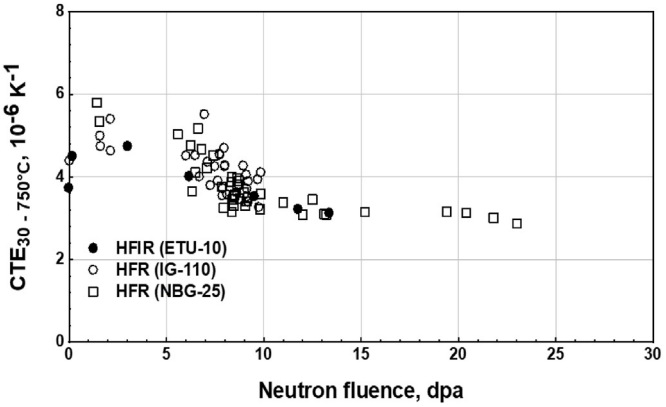

Fig. 7. Comparison of the CTE-dpa data of the HFIR (ETU-10) [8], the HFR (IG-110) and the HFR (NBG-25) [10]. The un-irradiated CTE data: ETU-10: $3.8X10^{-6}K^{-1}$, IG-110: $4.5X10^{-6}K^{-1}$, NBG-25: $3.9X10^{-6}K^{-1}$. Irradiation temperature: HFIR (ETU-10): 598°C, HFR (IG-110) and HFR (NBG-25): 750 °C

The thermal expansion of polygranular graphite is known to be controlled by the thermal closure of aligned internal porosity [21]. Thus, the CTE of graphite can be changed during irradiation at high temperature that accompanying pore microstructure changes at higher irradiation temperature. If the pore microstructure of the three graphite grades employed here is predicted to be similar, similar irradiation-induced changes in the CTE can be expected. The similar irradiation-induced changes in CTE observed in the HFIR (IG-110, 2017) (TR, 588 °C measured temp.) and HFIR (ETU-10) (TR, 598 °C irr. temp.), and among the HFIR (ETU-10), HFR (IG-110) and HFR (NBG-25) in Figs. 6 and 7, respectively, may thus be attributed to the similarities in the grades' microstructural responses to irradiation. In Fig. 7, if the ETU-10 was included in the HFR (INNOGRAPH project) irradiation, thus, the HFR (ETU-10) (irr. temp: 750 °C) was prepared, or if the HFIR (ETU-10) was irradiated at 750 °C, i.e., at about 150 °C higher than the HFIR (ETU-10) (irr.temp: 598 °C), both the HFR (INNOGRAP project, ETU-10) (irr. temp: 750 °C) and HFIR (ETU-10) (irr. temp: 750 °C) will show CTE changing behaviors more similar to the HFR (IG-110) and the HFR (NBG-25) in Fig. 7 since the CTE increases with increasing temperature [17].

5. Conclusion

The irradiation-induced dimensional and property changes of three fine-grained, iso-molded nuclear graphite grades, ETU-10, IG-110, and NBG-25, were compared based on irradiation-induced changes in volume (VC), thermal conductivity (TC), dynamic young's modulus (DYM), and coefficient of thermal expansion (CTE). The following results were obtained.

(1) Overall, the three grades showed similar irradiation-induced property changes and behaviors, which also followed the historic data trend. However, more or less, the VC and TC tended to show grade-sensitive changing behaviors and the DYM and CTE tended to show similar grade-insensitive changing behaviors, respectively.
(2) The ETU-10 of the smallest grain size appeared to show a relatively smaller VC among the grades. Drastic decrease in the difference in TC was observed for ETU-10 and IG-110 after irradiation. The observed similar irradiation-induced thermal conductivity decreasing behaviors between the ETU-10 and IG-110 suggest a similar irradiation-induced stable defect (which acts as phonon-scatter that decreases TC) formation behavior between the grades
(3) The similar irradiation-induced properties changing behaviors observed in this study especially in the DYM and CTE may be attributed to the assumed similar microstructures that evolved from the similar size coke particles and the same forming method.

Declaration of competing interest

The authors declare that they have no known competing financial interests or personal relationships that could have appeared to influence the work reported in this paper.

Acknowledgement

This study has been performed as a part of study for the graphite moderation small modular reactors in GINIS. The author wishes to acknowledge Mr. Hiroshi Okuda and Mr. Jun Ohashi, Ibiden, for their help in obtaining the data and reports employed in this study.

References

[1] Advances in Small Modular Reactor Technology Developments, IAEA, September, 2020.
[2] Overview of Small Modular Reactor Technology Development, Frederik Reitsma, IAEA Webinar, 29 July 2020.
[3] T.D. Burchell, in: T.D. Burchell (Ed.), Carbon Materials for Advanced Technologies, Chapter 13, Pergamon, UK, Oxford, 1999, pp. 429–484.
[4] S. Ishiyama, T.D. Burchell, J.P. Strizak, M. Eto, J. Nucl. Mater. 230 (1996) 1–7.
[5] A.A. Campbell, Y. Katoh, A.P. Selby, M. Yamaji, T. Konishi, High Dose Irradiation Behavior of IG-110, INGSM-18, Sept. 18-21, 2017. Baltimore, Maryland, USA.
[6] A. A. Campbell, Y. Katoh, M. Yamaki, T. Konishi, Effects of Neutron Irradiation at Elevated Temperatures on the Materials Properties of IG-110 (to be published in journal article).
[7] A.A. Campbell, Y. Katoh, Report on Effects of Irradiation on Material IG-110, ORNL/TM-2017/705, Nov. 2017.
[8] Y. Katoh, A.A. Campbell, A.P. Selby, T. Takagi, H. Kato, Results of High −Fluence Neutron Irradiation on Ibiden Nuclear Graphite ETU-10, INGSM-18, Sept. 18-21, 2017. Baltimore, Maryland, USA.
[9] A. A. Campbell, Y. Katoh, T. Takagi, H. Kato, Materials Property Changes in ETU-10 Due to Neutron Irradiation at Elevated Temperatures (To Be Published in Journal Article).
[10] M.C.R. Heijna, S. de Groot, J.A. Vreeling, J. Nucl. Mater. 402 (2017) 148–156.
[11] ASTM D 7219-08, Standard Specification for Isotropic and Near Isotropic Nuclear Graphite, ASTM, 2008.
[13] Gerd Haag, Thermal Conductivity of Graphite at High Fast Neutron Fluences, 3rd International Nuclear Graphite Specialist Meeting (INGSM-3), Oct. 19-22, Parma, Ohio, USA, 2002.
[14] NGNP High Temperature Materials White Paper, August 2012, INL/EXT-09-17187, vol. 1, Rev., August 2012, p. 41.
[15] T.D. Burchell, Chapter 4.10, radiation effects in graphite, in: Rudi Konings (Ed.), Comprehensive Nuclear Materials, vol. 4, Elsevier Ltd. Oxford, 2012, pp. 299–324, pp. 311-312.

[16] T.D. Burchell, W.P. Eatherly, J. Nucl. Mater. 179–181 (1991) 205–208.
[17] R.E. Nightingale, H.H. Yoshikawa, H.H.W. Losty, Chapter 6, physical properties, in: R.E. Nightingale (Ed.), Nuclear Graphite, Academic Press, New York, 1962, pp. 117–186.
[18] Mike Davies, Assessment of Candidate Graphites for Future High Temperature Reactors, INGSM-13, Meitingen, Germany, 2012. Sept. 23-26.
[19] M.C.R. Heijna, J.A. Vreeling, S. de Groot, Comparison of Irradiation Behavior of HTR Graphite Grades, INGSM-18, Baltimore, Maryland, USA, 2017. Sept. 18-21.
[20] L.L. Snead, J. Nucl. Mater. 381 (2008) 76–82.
[21] Pergamon, LondonT.D. Burchell (Ed.), Carbon Materials for Advanced Technologies, 1999, pp. 205–208, 465.

Further reading

[12] P. Wang, C.I. Contescu, S. Yu, T.D. Burchell, J. Nucl. Mater. 430 (1–3) (2012) 229–238.